AMES GRANT
IN-45-CR
13489
P37

FIRST SEMIANNUAL PROGRESS REPORT

TO: NATIONAL AERONAUTICS AND SPACE ADMINISTRATION
AMES RESEARCH CENTER

FROM: NORTH CAROLINA STATE UNIVERSITY, RALEIGH, NC 27695

FOR: **"HETEROGENEOUS PHOTOCATALYTIC OXIDATION OF ATMOSPHERIC TRACE CONTAMINANTS"**
NASA RESEARCH GRANT 2-684

BY: DAVID F. OLLIS AND JOSE PERAL
CHEMICAL ENGINEERING DEPARTMENT
NORTH CAROLINA STATE UNIVERSITY
RALEIGH, NC 27695
PHONE: (919)-737-2329
FAX: (919) 737-3465

PERIOD COVERED: 11/1/90 THROUGH 4/30/91

PRINCIPAL INVESTIGATOR:

DAVID F. OLLIS, PROFESSOR

SUBMITTED: 5/15/91

TABLE OF CONTENTS

List of Tables ii

List of Figures iii - v

Summary 1

I. Photoreactor design 3

II. Reactant class #1: Ketones 4
- a) catalyst conditioning 4
- b) rate vs. acetone concentration 4
- c) rate variation with intensity; quantum yield of reaction 5
- d) inhibition by water 7
- e) summary: actone results 7

III. Reactant class #2: Alcohols 8
- a) catalyst conditioning 8
- b) rate variation with n-butanol concentration 8
- c) rate dependence on water vapor content 9

IV. Photocatalyst deactivation 9
- a) influence of n-butanol on deactivation 9
- b) deactivation influence of water 10
- c) catalyst reactivation 12
- d) influence of temperature on deactivation 13
- e) long term ambient temperature illumination 13

V. Future Work 13

VI. Nomenclature 15

VII. References 16

VIII. Tables 17-20

IX. Figures 21-31

LIST OF TABLES

1. Summary of Projected Trace Contaminant Generation Rates

2. Scope of Experimental Program and Reactor Design Study

3. Catalyst Deactivation and Activity Recovery

LIST OF FIGURES

		Page
FIGURE 1:	Schematic of first experimental system for study of photocatalytic air purification: single gas supply configuration	21
Figure 2:	Second experimental system for photocatalytic air purification: dual gas reservoir feed configuration.	22
Figure 3:	Percent of feed acetone adsorbed vs. time: dark conditions, feed acetone concentration = 243.5 mg/m^3 (time in minutes).	22
Figure 4:	Reciprocaln rate vs. reciprocal acetone concentration: photocatalyzed conversion of acetone on illuminated TiO_2.	23
Figure 5:	Acetone reaction rate (left) and apparent quantum yield (right) vs. irradiance.	23
Figure 6:	Rate of reaction vs. irradiance: acetone conversion at constant feed concentration .	24
Figure 7:	Quantum yield vs. irradiance; acetone conversion at constant acetone feed concentration.	24
Figure 8:	Rate of acetone photocatalyzed oxidation vs. feed water vapor concentration; acetone feed concentration = constant.	25

Figure 9: Percent butanol adsorbed vs. time of air/n-butanol flow; dark conditions. 25

Figure 10: Reciprocal rate of butanol conversion vs. reciprocal of butanol feed concentration. 26

Figure 11: Butanol reaction rate(left) and buteraldehyde formation rate(right) vs. water vapor content of feed. 26

Figure 12: Butanol percent reacted (left) and product formed as percent of butanol fed (right) vs. reaction time; time of dark periods not included. (Feed butanol = 260 mg/m^3) 27

Figure 13: Butanol percent reacted (left) and products formed as percent of butanol fed (right) vs. reaction time; dark time period not shown. (Feed butanol concentration = 140 mg/m^3) 27

Figure 14: Deactivation: Percent butanol converted vs. time of reaction. 28

Figure 15: Deactivation: Percent of butanol removal and percent of buteraldehyde formed vs. reaction time. 28

Figure 16: Deactivation: Percent butanol converted and percent of buteraldehyde formed vs. reaction time. 29

Figure 17: Deactivation: Percent butanol reacted and buteraldehyde formed vs. reaction time. 29

Figure 18: Test for dark reaction activity: percent of butanol reacted (left) and percent of buteraldehyde formed(right) vs reaction time. 30

Figure 19: Influence of temperature on deactivation: percent butanol converted and buteraldehyde formed vs. reaction time at 75-80^{o}C. 30

Figure 20: Effect of temperature on deactivation: conversion of butanol and formation of buteraldehyde vs. reaction time: T = 61-62^{o}C. 31

Figure 21: Long time irradiation: butanol conversion and buteraldehyde formation vs. reaction time. T = 22-25 ^{o}C. 31

SUMMARY:

A two year study to examine the feasibility of using heterogeneous photocatalysis for spacecraft air purification was begun at NCSU on November, 1, 1990. The original grant proposal included examination of the rates of destruction of anticipated spacecraft generated air contaminants, including alcohols, aldehydes, chlorinated compounds,as well as trace levels of volatile compounds containing nitrogen, sulfur, and silicon.

In the first six month period of 11/1/90 to 4/30/91,the following items were demonstrated or explored:

(a) Design and construction of continuous flow photoreactor for study of oxidation of trace atmospheric contaminants

Results:

- operational photoreactor

(b) Establishment of kinetics of acetone oxidation including adsorption equilibration, variation of oxidation rate with acetone concentration and water (inhibitor), and variation of rate and apparent quantum yield with light intensity

Results:

- rate follows Langmuir-Hinshelwood form with k = 1.07 $\mu g/cm^2$-min and K = $5.92.10^{-3}$ m^3/mg
- rate varies as $(intensity)^{0.73}$
- quantum yield declines as $(intensity)^{-.27}$
- water vapor inhibits rate as $(water)^{-1.7}$

(c) Exploration of kinetics of butanol oxidation, including rate variation with concentration of butanol, and lack of inhibition by water.

Results:

- rate follows Langmuir-Hinshelwood form with k = 39 $\mu g/cm^2$-min and K = $5.46.10^{-4}$ m^3/mg
- rate independent of water vapor concentration

(d) Exploration of kinetics of catalyst deactivation during oxidation of butanol, including deactivation rate, influence of dark conditions, and establishment of photocatalytic regeneration of activity in alcohol-free air.

Results:

- catalyst deactivation is strong with n-butanol
- water has only minor influence on deactivation rate
- catalyst can be photoreactivated in alcohol-free air
- temperature has minor influence on catalyst photodeactivation rate

The second six month period will include initial screening of all remaining reactant classes, design of a laboratory scale recirculating reactor configuration, and initiation of a fundamental engineering analysis of the coexisting illumination, concentration and flow fields in the operating photoreactor.

I PHOTOREACTOR DESIGN: Flow photoreactors for gas-solid heterogeneous photocatalysis have been constructed previously in several laboratories, including those of Teichner et al (1) in France, Raupp (2) , Dranoff (3) and Griffin (4) in the US, and Gratzel (5) in Switzerland. For the present study, the flat porous glass frit on which a thin layer of active photocatalyst powder could be supported was found useful; our reactor configuration shown in Figure 1 is essentially that of Teichner and Raupp.

Our first system configuration (Figure 1) allows for a given reactant, such as acetone, to be injected in liquid form with a microsyringe into a slightly pressurized , UHP air-filled reservoir; following sample evaporation, the resulting reservoir of slightly contaminated air is available for flow over the illuminated photocatalyst. In operation, the mass flow controller is set to provide a constant mass flow rate of lightly contaminated air to the photoreactor. Temperature is monitored by a thermocouple located just below the photocatalyst ; illumination intensities achieved with the 100 watt blacklight were such as to provide nearly ambient temperature operation. The trace level of contaminant was insufficient to generate any appreciable heat of reaction. This reservoir configuration allowed for runs of up to one or two hours, easily adequate for acetone conversion studies (see (II) below) and a constant activity catalyst.

A recent system modification (Figure 2) ,allowing for longer runs, includes the provision of a more concentrated reactant/air reservoir, which is slowly bled into a continuous UHP air feed from a high pressure cylinder. This dual feed configuration we found useful for catalyst deactivation studies (see section (IV) below where a single run may last for hours.

In each system, gas sampling loops are positioned to allow capture of aliquots of either the reactant feed or the product stream; these samples are fed directly to a gas chromatograph operating with a flame ionization detector. This level of detection is adequate for assays at 1% to 100% levels of the Spacecraft Maximum Allowable Concentrations (SMAC) for the reactants to be examined in this study (see Table 1).

II REACTANT CLASS #1 KETONES : ACETONE.

The research program includes examination of ketones, aldehydes, alcohols, etc. as shown in Table 2. The first reactant selected was the ketone acetone, known to be an intermediate in the previously reported photocatalytic partial oxidation of isobutane under hydrocarbon rich conditions (Teichner et al (6)), and for which no subsequent intermediates had been reported. Thus, we anticipated that this might provide a simple kinetic behavior, for which the acetone in air would be directly converted to carbon dioxide and water, with no or minimal intermediates .

a. Catalyst conditioning. Both the catalyst and the glass frit have an appreciable surface area, which for normal catalyst studies involving reactant partial pressures of 0.1 to several atmospheres, would be expected to come rapidly to a gas-solid equilibrium in a flow reactor. With an only slightly contaminated air feed, however, the surface inventory of strongly held reactant requires some time to accumulate and eventually reach a "dark" gas-solid equilibrium; Consequently, the trace contaminated air to be examined must first be fed for several hours until the feed and reactor exit gas concentrations are identical. This initial conditioning of the adsorbed phase with trace acetone in air is shown in Figure 3, which indicates that after just over two hours, the feed and exit acetone concentrations were identical, and the photocatalyst measurements could begin. Measurements at earlier times would have mistakenly included an apparent acetone loss term which only represents adsorption, not reaction. This conditioning requirement had not been remarked on by previous investigators.

(b) Rate vs. acetone concentration. Following achievement of equal acetone levels in the feed and exit, the illumination was begun, and a run was terminated when the exit acetone reached a new steady value on repeated samplings. The reaction rate variation with reactant acetone was first plotted as reciprocal rate vs reciprocal of acetone feed concentration, as this plot should be linear if the rate followed a conventional Langmuir-Hinshelwood equation of the form of equation (1):

$$\text{Rate} = k\,K\,(\text{Reactant})/(1. + K\,(\text{Reactant})) \quad (1)$$

Thus, inversion gives equation (2),

$$1/(\text{Rate}) = (1/k) + 1/(k\,K\,x\,(\text{Reactant})) \quad (2)$$

which is tested by plotting reciprocal rate vs. reciprocal concentration. When the reactant conversion is modest, the concentration throughout the bed is nearly uniform, and the flow-through configurations of Figures 1 and 2 can be analyzed with equation (2).

Such a plot of the data is shown in Figure 4 for acetone. This nicely linear form of the data validates the use of equation (2) for predicting acetone degradation rates. The values of the rate constant k and the pseudo-adsorption constant K are found from Figure 4 to be:

$k = 1.07\ \mu g/cm^2\text{-}min$

$K = 5.92 \times 10^{-3}\ m^3/mg$

No other organic species were noted by the flame ionization detector. While this detector is sensitive to any vapor phase component with a modest or higher heat of combustion, it may not detect formic acid (HCOOH). Prior photocatalytic studies have demonstrated that formic acid is rapidly converted to carbon dioxide and water (6). We conclude that acetone is cleanly converted to carbon dioxide and water under the trace feed levels appropriate to expected spacecraft air conditions (7).

(c) Rate variation with intensity; quantum yield of reaction:

The photocatalyzed oxidation reaction is expected to be intensity dependent, as reflected in prior literature. Liquid phase studies have reported first order dependence of rate on intensity at low light levels (less than one sun near UV equivalent or approximately 5.10^{14} photons/cm^2-sec) (Egerton and King (7) and Okamoto et al(8)) and half order dependence above one sun near UV equivalent, as found

by Egerton and King (7), Okamoto et al (8), Kornmann et al (9), and D'Oleivera et al (10).

Our rate vs. intensity data for acetone are shown in Figure 5. The rate increases less rapidly than first order, and more rapidly than half-order. We are in the transition regime noted earlier by Okamoto et al (8). The apparent fractional dependence of rate on intensity is given by equation (3):

$$\text{Rate} = k' \times (\text{Irradiance})^{a}, \qquad (3)$$

where $a = 0.73$, evaluated from the slope of ln (Rate) vs. ln (Irradiance) in Figure 6.

The efficiency of utilization of light to drive the desired oxidation reaction is represented by the apparent quantum yield, q , defined in equation (4):

q = (reaction rate (molecules per time)/(photon absorption rate(photons per time)) (4)

This quantum yield definition is convenient, but not fundamental, as the conversion acetone to carbon dioxide is clearly a multi-step, multi-photon process and may involve dark steps in the mechanism as well. However, the apparent quantum yield, as defined above, is important for overall reaction kinetics and for later economic estimates of process costs.

The apparent quantum yield is also plotted vs. irradiance in Figure (5). For a processs first order in irradiance, the quantum yield would be constant. For a half-order rate dependence on irradiance, the quantum yield would vary inversely with the square root of irradiance, i.e., exhibit a -0.5 order. Figure (5) again indicates a transition behavior, as a semilog plot (Figure 7) indicates that q varies approximately as equation (5):

$$q = q' (\text{Irradiance})^{b} \qquad \text{where } b = -0.27 \qquad (5)$$

(d) Inhibition by water: Water is a product of the stoichiometric oxidation of acetone by oxygen:

$$CH_3COCH_3 + 4O_2 \rightarrow 3CO_2 + 3H_2O \quad (6)$$

The influence of water on the rate of photocatalyzed reactions is reactant dependent. Thus Dibble and Raupp (2) found the rate of trichloroethylene conversion to be zero order for water mole fractions below 10^{-3}, and to become strongly inhibitory, exhibiting a -3 order dependence for water vapor phase mole fractions between 5×10^{-3} and 5×10^{-2} In contrast, Suzuki et al (12) found that toluene photocatalyzed oxidation was enhaced by water vapor, increasing almost linearly with water vapor content between 0% and 60% relative humidity . Interestingly, water is a reactant for TCE conversion and a product for toluene conversion:

$$CHClCCl_2 + H_2O + 2O_2 \rightarrow 2\,CO_2 + 3\,HCl \quad (7)$$

$$C_6H_5CH_3 + 8\,O_2 \rightarrow 6\,CO_2 + 4\,H_2O \quad (8)$$

Oxygen adsorption on titanium dioxide is known to depend on the surface density of hydroxyl groups(13), which in turn are provided by water. The rationalization for these contradictory influences of water awaits a fuller understanding of surface mechanisms which will be sought in later experiments.

We find that the oxidation of acetone is inhibited by variations of water vapor pressure in the feed reservoir, as shown in Figure 8. The apparent dependence of rate of water mole fraction (or concentration) is given by

$$\text{Rate} = k''\,(\text{water})^c, \qquad \text{where } c = -1.7 \quad (9)$$

(e) Summary: For acetone, oxygen and water vapor concentrations expected in spacecraft and under our illumination levels, the rate of the complete oxidation of acetone into carbon dioxide and water is Langmuirian as regards acetone, inverse 1.7 order in water, and varies as irradiance raised to the +.70 power.

We note that the oxygen level rests essentially constant under all anticipated conditions (enormous excess), and that any oxygen dependence of the rate is irrelevant for this application. The water vapor level will be that represented by the spacecraft conditions, e.g., 10-80% relative humidity under ambient temperature conditions; this represents an enormously larger amount of water than can be created or consumed in any photocatalytic reaction for the contaminant levels indicated in Table 1. Water vapor content is thus a given quantity, and the photocatalytic reactor of eventual design must achieve the desired conversions even under the least favorable water conditions.

III. Reactant Class #2 : Alcohols : n-Butanol. Alcohols are expected spacecraft contaminants (Table 1: ethanol, propanol, n-butanol(1-butanol), cyclohexanol, etc). The first alcohol examined was n-butanol (1-butanol).

(a) Catalyst conditioning. As with acetone, in the absence of light a considerable time period was required to achieve a reactor exit concentration equal to the feed value (Figure 9). The quantity of n-butanol adsorbed by the conbination of the phtocatalyst and the glass frit was 2.01 mg vs. a value of 0.206 mg for acetone. Upon reaching a dark equilibrium, the near-UV source was illuminated, and the photocatalytic studies begun.

(b) Rate variation with n-butanol concentration: A plot of inverse rate vs. inverse n-butanol concentration is linear for the first four data points in Figure 10, indicating that the Langmuir-Hinshelwood form is again useful. The rate and apparant binding constants for these data are

$k = 39.\ \mu g/cm^2\text{-}min$

$K = 5.46 \times 10^{-4}\ m^3/mg$

When reaction is commenced, the catalyst activity diminishes for some time before reaching an apparently constant value. The far right point in Figure 10 was the first measurement taken; the remainder correspond more closely to constant but diminished

activity. The Langmuirian behavior thus appears to describes the partially deactivated catalyst. Catalyst deactivation is discussed below in section (IV).

(c) Rate dependence on water vapor content: Figure 11 indicates that variations in water vapor content has no important effect on the rate of disappearance of n-butanol. A very modest decline of conversion of n-butanol is noted in the data, and the concentration of the single product buteraldehyde is also seen to be unaffected by the water vapor content.

Thus, we have the following information as regards the water vapor dependence of the rate of gas-solid, photocatalyzed oxidation of trace contaminants:

trichloroethylene: water is a rate inhibitor (2)
acetone: water is a rate inhibitor (present study)

n-butanol : water is neither an inhibitor nor a promoter (present study)

toluene: water is a rate promoter(12)

These differing by three different laboratories all apply to trace contaminant oxidation in air at ambient temperatures using titanium dioxide photocatalysts which are predominantly anatase (most active) phase.

IV Photocatalyst deactivation :

(a) Influence of n-butanol on deactivation: Initiation of n-butanol photocatalyzed oxidation resulted in very high initial disappearance rate of n-butanol and a rapid rise in appearance of a product identified as buteraldehyde.(Figure 12). Trace amounts of a second product, probably butene , were also noted. With time, butanol conversion decreased markedly until a constant conversion of about 30% was reached between 100 and 200 minutes. Following a dark condition at 200 minutes, during which the reactant flow was continued, re-illumination again resulted in a further deactivation to a new, constant activity of about 18-19% conversion. A subsequent dark period and re-illumination produced yet a third step

deactivation to a new steady level.

The existence of photocatalyst deactivation by alcohols was reported long ago by Cunningham and Hodnet(13). These authors examined the photocatalyzed oxidation of 2-butanol and 2-propanol (1-propanol is another anticipated contaminant, Table 1) over illuminated titanium dioxide and zinc oxide. Similar time deactivation profiles were seen; these authors used much higher pressures of alcohol, e.g., 8 mm Hg of 2-butanol (about 25,000 ppm), while we observed inhibition at 160-260 mg/m^3 (or about 120-200 ppm). These authors suggested that carbon dioxide products could be bound to the surface and thereby deactivate or block some sites. Rate data for CO_2 and ZnO was presented which was consistent with this hypothesis, but no data or reference to titanium dioxide was offered. We are not aware of any other authors examining photocatalytic oxidations who have reported such catalyst deactivation for any other reactants until our n-butanol results.

Since all oxidations produce carbon dioxide, a more likely explanation of this deactivation peculiar to alcohols is that adsorbed alcohols are able to effect a particular deactivation or site blockage which reflects an initial transient only , since a constant activity is reached in each case after dark exposure to the feed. The nature of this adsorbed material is combustible under appropriate conditions, since the catalyst may be regenerated photocatalytically in pure air as we discuss below in section (c) .

This deactivation was also observed at lower concentrations of n-butanol (Figure 13, 140 mg/m^3 feed butanol). Again, new steady states were noted, as indicated by the data between 45 and 135 minutes, 165-225 minutes, and 285-360 minutes. In both Figures, deactivation is observed transiently only after a dark period during which n-butanol adsorption from a flowing gas phase is allowed. It will be interesting to see if deactivation can be avoided by catalyst start-up in UHP with illumination, followed by commencement of flow of the simulated contaminated air. These experiments arepart of the effort planned for the second six month period.

(b) Deactivation influence of water: Figures 12 and 13 correspond to feed water contents of about 1,000 mg/m^3, included as a reference concentration because spacecraft air is expected to

have a finite, controlled humidity. When water was entirely absent from the feed, the loss of catalyst oxidation activity was continual and of anearly linear shape for a first, long period, as shown in Figure 14. Repeat runs with the same catalyst and nearly the same concentrations of reactant (Figures 15-17) showed similar continuous deactivations. The continuing loss of activity here is reminiscent of a remark by Dibble and Raupp(2) who noted that for TCE photocatalyzed conversion, a water-free feed led ultimately to a complete loss of rate of oxidation reaction. Their loss could have occured for at least two different reasons:

(1) The TCE conversion had a stoichiometric need for water as a reactant (recall equation (6) above), since additional hydrogen is needed for formation of HCl from the highly chlorinated reactant.

(2) The surface could have become exhausted of hydroxyl groups, required for oxygen adsorption (13), due to lack of water to replenish them.

Thus their rate loss of rate could have arisen from exhaustion at the surface of either water as a stoichiometric reactant or as an oxygen-assisting adsorbate. If adsorbed hydroxyls function as traps for photoproduced holes (h+) , then each hydroxyl allows for formation of one O_2^- species by reaction of O_2 with the stoichiometric photoproduced electron (e-), and the two possible explanations become one and the same.

In our case, the n-butanol will form water upon complete oxidation. The question which arises is: are we achieving complete oxidation for the conditions in Figures 14-17? We will explore this further with mass spectrometric analyses in the second six month period.

A major apparent intermediate, buteraldehyde, is always present during the conversion of n-butanol. This product may have arisen from a simple dehydrogenation,

$$CH_3CH_2CH_2CH_2OH \quad ---> \quad CH_3CH_2CH_2CHO + H_2 \qquad (10)$$

or an oxidative dehydrogenation,

$$CH_3CH_2CH_2CH_2OH + (1/2)\ O_2 ---> CH_3CH_2CH_2CHO + H_2O \qquad (11)$$

Since the flame ionization detector operates on a hydrogen-oxygen flame, hydrogen is the one combustible item which may not be detectable via FID.

We consider the possibilities, and future tests to discriminate among them:

(1) Water has ceased to be produced altogether. This reduces the oxidative activity which requires molecular oxygen, because water cannot now regenerate the surface hydroxyl groups (It loses in competitive adsorption with n-butanol), and molecular oxygen is no longer taken up by the illuminated catalyst. This can be tested by used of a deuterated reactant and mass spectrometric analysis for formation of D_2O.

(2) Water is generated in reaction (11), but cannot rehydroxylate the surface because n-butanol adsorbs too strongly. This can be tested with the same experiment as above..

(3) The conversion of n-butanol to buteraldehyde is actually a dark reaction. In this case, the loss of butanol conversion continues until the butanol conversion matches the buteraldehyde generated. This would correspond to a 100 % inactivation of the photocatalyst oxidation activity, leaving only a residual dark activity for dehydrogenation. Dark reaction tests were recently carried out; this possibility was ruled out, however, as no buteraldehyde was observed with feed in the dark (no reaction: Figure 18). Thus the remaining activity for conversion of n-butanol to buteraldehyde is also a photocatalyzed reaction: the oxidation activity has diminished, but the dehydrogenation activity remains.

(c) Catalyst reactivation: A series of pretreatments for the catalyst is summarized in Table 3, along with the resultant initial activity. Replacement of the flow of contaminant-bearing air by pure air and continued ilumination for varying periods of time results in a progressive regeneration of catalyst activity, ultimately reaching to or near the original level of photocatalytic oxidation(Table 3). This data shows clearly that catalyst pretreatment of illumination in UHP air feed results in catalyst activity regeneration. There remains also the possibility that if illumination in pure air is commenced before the flow of reactant is first begun, that the deactivation can be avoided; this possibility will be tested.

(d) Influence of temperature on deactivation: Operation at different temperatures of 75-80 ^{o}C and 61-62 ^{o}C was examined to see if deactivation was increased or decreased under such conditions. Each new temperature again produced a transient deactivation period , which ultimately reached a "plateau" activity at which all n-butanol converted appear exclusively as product buteraldehyde. (Figures 19 and 20)

(e) Long term ambient temperature illumination: Operation at ambient temperature for long times (6 hours) in the presence of water produced no further trends (Figure 21); activity for photocatalyzed conversion of butanol to buteraldehyde appears constant, and photocatalytic oxidation to carbon dioxide appears to be absent. This presumption will be checked with the added use of mass spectrometric analysis as mentioned previously. .

FUTURE WORK
(NEXT SIX MONTHS)

1. Complete testing of at least one compound from each contaminant structure group:

group	example contaminant
aromatics	m-xylene
chlorinated hydrocarbon	methylene chloride
nitrogen heteroaromatic	2,3-benzopyrrole
aliphatic	methane
fluorinated hydrocarbon	Freon
siloxane	silane

2. Examine influence of start-up sequences on deactivation

3. Initiate photocatalyst detailed design study

4. Initiate photoreactor system first prototype design and construction

NOMENCLATURE

a = reaction order in irradiance

b = quantum yield order in irradiance

c = reaction order in water

Einstein = mole equivalent ($6.023.10^{23}$) of photons

k = photocatalyst rate constant ($\mu g/cm^2$ catalyst-min)

K = photocatalyst adsorption pseudo-equilibrium constant (under illumination) $(mg/m^3)^{-1}$

q = apparent quantum yield
($\equiv$ reaction rate/photon absorption rate)
(molecules/photon)

SMAC = Spacecraft Maximum Allowble Concentration

REFERENCES

1. Formenti, M., F. Juillet, and S. J. Teichner, C. R. Acad. Sci., Paris, C270(1970)138.

2. Dibble, L. A., and G. Raupp, Proc. Ariz. Hydrogeol. soc., First Annual Symp., 221-229 (1988). Dibble, L. A. and G. Raupp, Catalysis Letters, 1990.

3. Ayoub, P. PhD thesis, Northwestern University, (1986). Ayoub, P. and J. Dranoff, AIChE Mtg., New York, Nov., 1987.

4. Blake, M. R. and G. Griffin, J. Phys. Chem., 92, 5897 (1988); Carlson, J. and G. Griffin, J. Phys. Chem., 90, 5896 (1986).

5. Thampi, K. R., J. Kiwi, and M. Gratzel, Catralysis Letters 1, 109 (1988).

6. Formenti, M. F. Juillet, and S. J. Teichner, Bull. Soc. Chim. Fr., 7-8, 1031(1976).

7. Sato, S., J. Chem. Soc., Chem. Commun., 26, 1986: J. Phys. Chem. 87, 3531 (1983).

8. Leban, M. J. and P. Wagner, Intersociety Conference on Environmental Systems, (ICES), San Diego, CA 7/24-26/89. Paper #891513.

9. Egerton, T. A. and King, C. J., J. Oil Col. Chem. Assoc., 62, 386 (1979).

10. Lkamoto, K., Y. Ysamamoto, H. Taneka, A. Itaya, Bull. Chem. Soc. Japan, 58, 2023 (1985).

11. Kornmann et al, Environmental Science, Technol., 1991.

12. D'Oleivera et al, Environmental Science and Technology, 1990.

13. Ibusuki, K. T. Yazawa, and T. Ibusuki, Atmos. Environ., 20, 1171 (1986).

14. Boonstra, A. H., and A. H. A. Mutsaers, J. Phys. Chem., 79, 1694 (1975).

15. Cunningham, J. and B. K. Hodnett, J. Chem. Soc. Far. Trans., 1, 77 (1981)

TABLE 1
Summary of Projected Trace Contaminant Generation Rates
(from Leban and Wagner (1989))

Major contaminant

Class	Contaminant	Projected Space Station Generation Rate (mg/day)
Alcohols:	ethanol	5,216
	2-propanol	2,022
	1-butanol	6,922
	cyclohexanol	1,288
	all others	1,677
	alcohol total	17,125
Aldehydes:	butanal	1,470
	all others	221
	aldehyde total	1,691
Ketones:	acetone	4,212
	methyl ethylketone	3,760
	methyl isobutyl ketone	1,335
	all others	1,920
		11,227
Aliphatic hydrocarbons:		
	methane	1,620
	all others	2,611
		4,231
Aromatic hydrocarbons:	toluene	1,351
	m-xylene	3,539
	all others	1,532
	total aromatics	6,422

TABLE 1 (continued):
Summary of Projected Trace Contaminant Generation Rates (after Leban and Wagner (1989))

Freons:	Freon 22	467
	Freon 113 (1,1,2-trichloro-1,2,-trifluoroethane)	9,180
	Freon TF (1,1,2-trichloro-1,2,2,-trifluoroethane)	13,801
	Total	23,448
Other Halocarbons:	methylene chloride	1,746
	chlorobenzene	1,240
	all others	3,493
	total of Other Halocarbons	6,479
Esters:	2-ethoxy-2-ethanol	1,035
	all others	3,067
	total esters	4,490
Silanes and Siloxanes:	total	2,470
Organic nitrogens:	indole(2,3-benzopyrrole)	25
	others	382
	total	407
Sulfides:	total	50
Miscellaneous organics:	total	6
Inorganics:	hydrogen	208
	ammonia	3,806
	carbon monoxide	1,843
	others	52
	total inorganics	5,909
Total organics		77,848
Total inorganics		5,909
	Total	83,757

TABLE 2
Scope of Experimental Program and Reactor Design Study

A. Summary of Experimental Program

I. Determination of Operating Conditions for 90+% conversion (12 months) (T= 65°F and T=80°F(spacecraft ambient min. and max.)

1) Pure component conversions:

hydrocarbons and oxygenates:	1-butanol, butanal, acetone, methane, m-xylene
halocarbons:	methylene chloride, Freon 113, Freon TF, Freon 22
silane, siloxane.	
2,3-benzopyrrole	
ammonia	
2) Model mixed feed:	ammonia, 1-butanol, acetone, m-xylene, methylene chloride, silane.

TABLE 3
Catalyst Deactivation and Activity Recovery

Day	Catalyst Pretreatment Conditions	[Butanol] (mg/m3)	Rate Butanol Oxidation (μg/cm2min)	Rate Butyrald. Formation (μg/cm2min)
1	Fresh Catalyst	132	2.38	1.98
19	After several Runs	125.8	1.48	1.2
22	Fresh air flow during 90 min (dark)	141	1.15	0.87
26	Fresh air flow overnight (dark)	150	0.929	0.70
39	Fresh air flow overnight (light)	151	1.88	1.23
67	Fresh air flow (74 °C and dark)	129.1	0.347	0.29
39	Fresh air flow overnight (light)	132.3	1.42	0.94
68	Fresh air flow (49 °C and dark)	126	0.561	0.298

[Water]≈1000 mg/m^3

EXPERIMENTAL SYSTEM

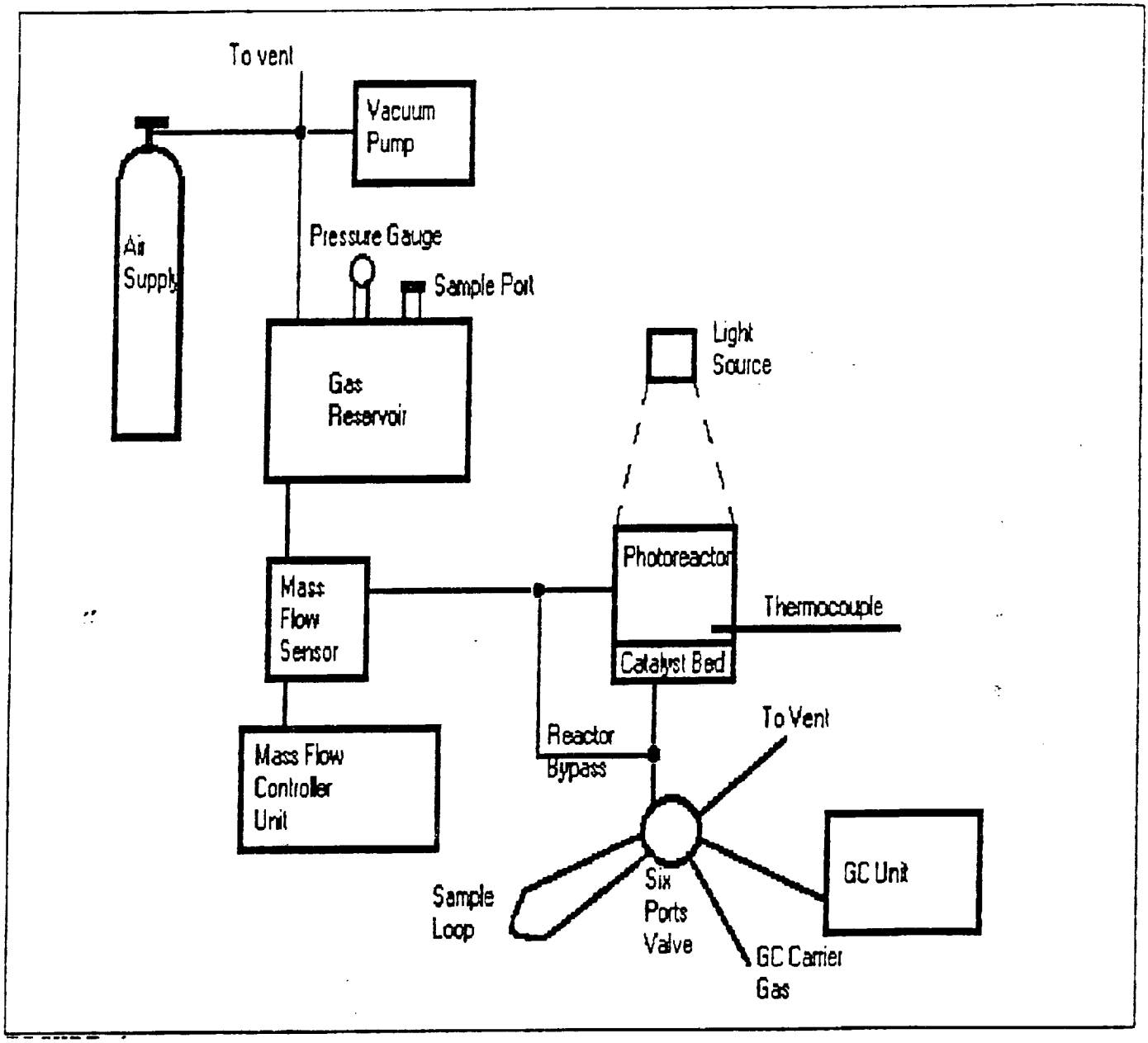

FIGURE 1: Schematic of experimental system 1 for study of photocatalytic air purification: single gas supply configuration

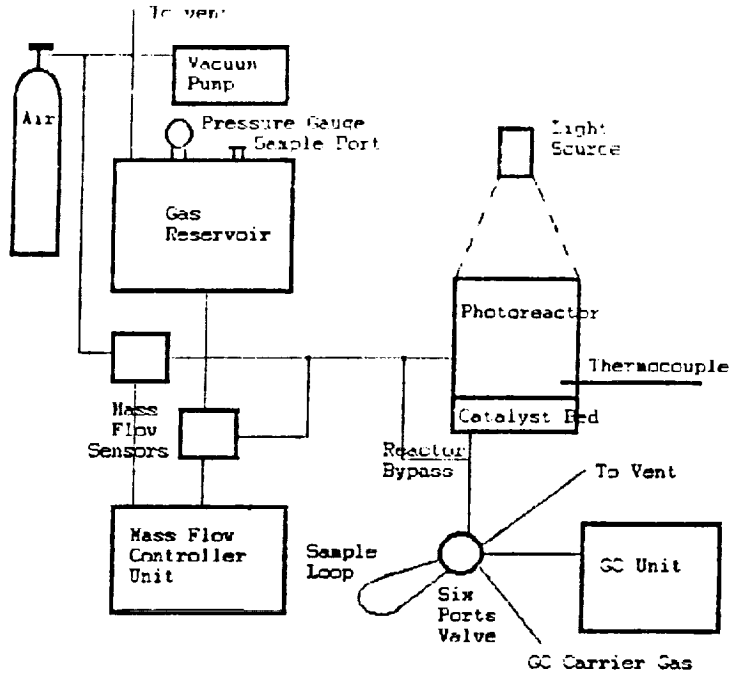

Figure 2: Second experimental system for photocatalytic air purification: dual gas reservoir feed configuration.

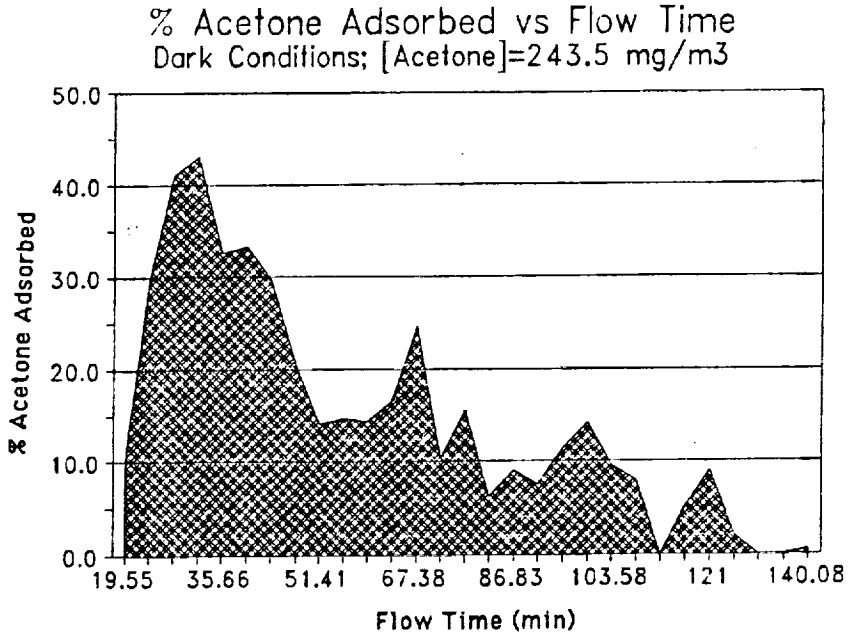

Figure 3: Percent of feed acetone adsorbed vs. time: dark conditions, feed acetone concentration = 243.5 mg/m^3 (time in minutes).

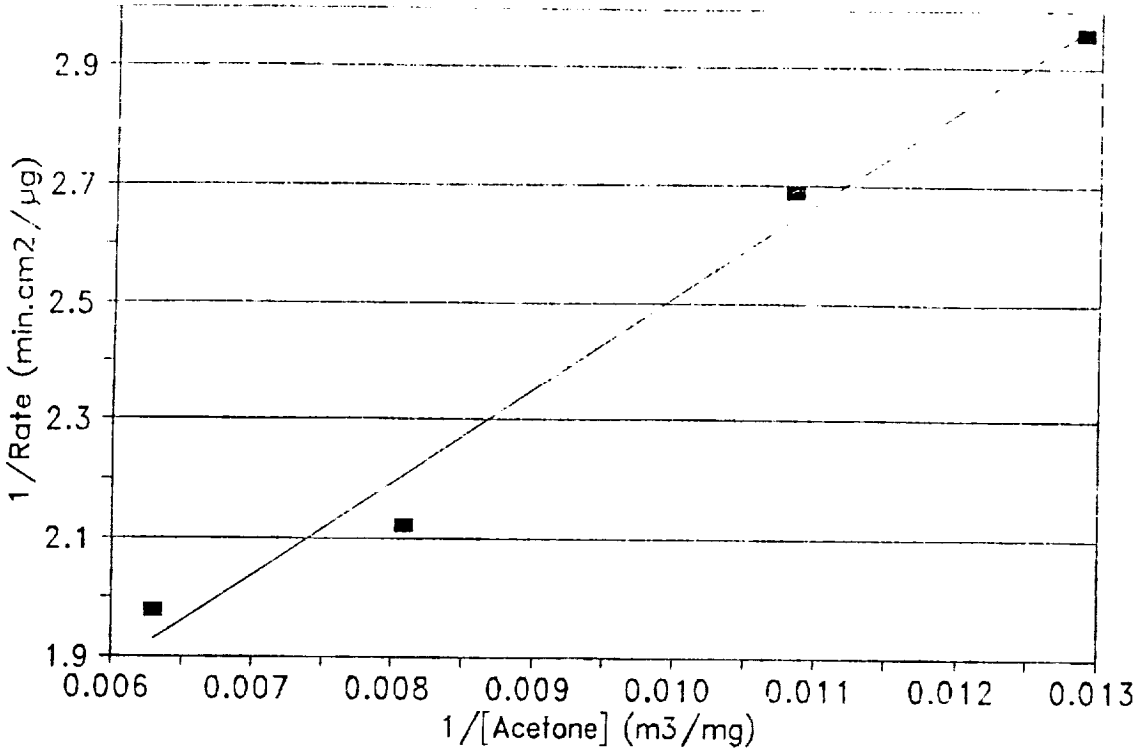

Figure 4: Reciprocal rate vs. reciprocal acetone concentration: photocatalyzed conversion of acetone on illuminated TiO_2.

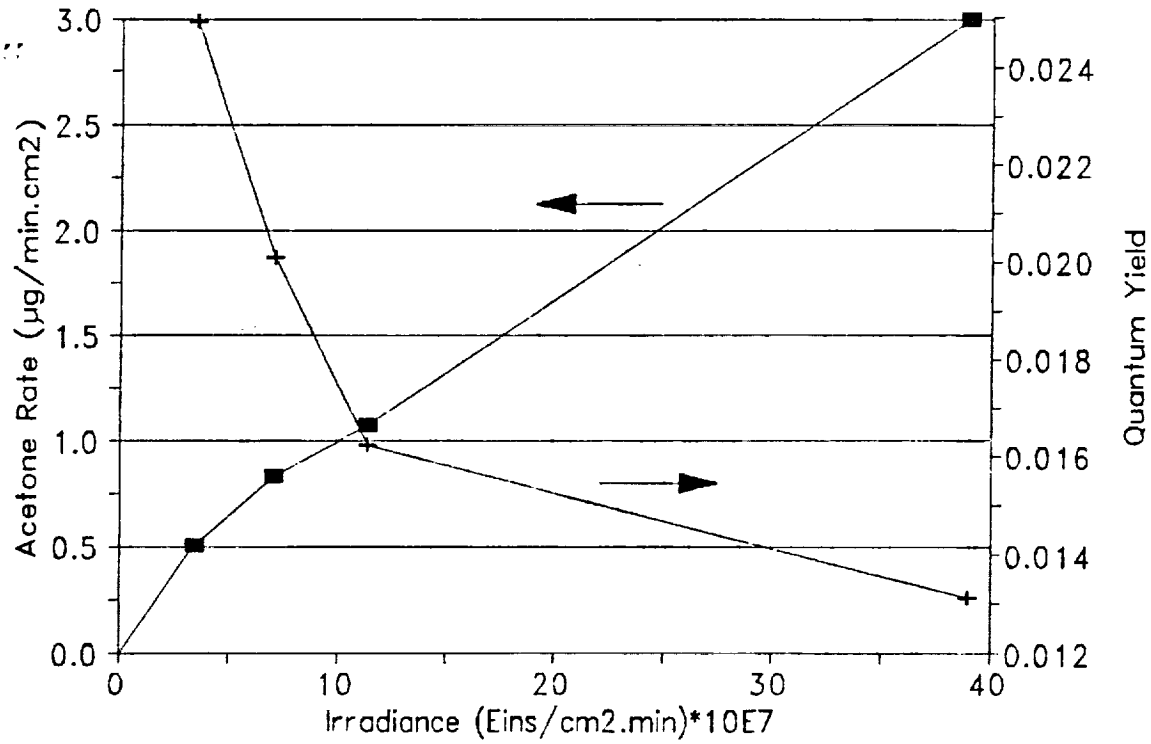

Figure 5: Acetone reaction rate (left) and apparent quantum yield (right) vs. irradiance.

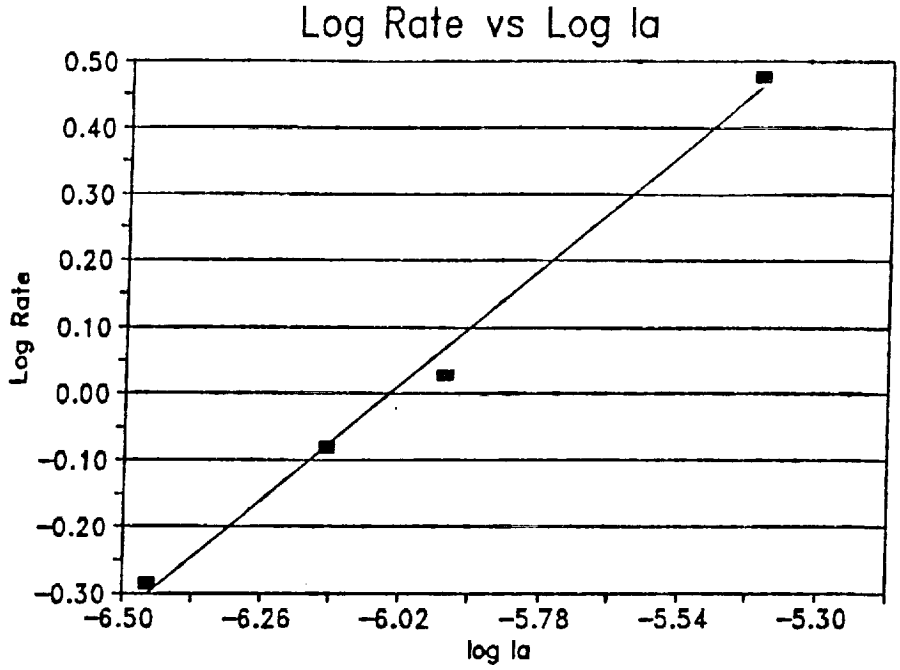

Figure 6: Rate of reaction vs. irradiance: acetone conversion at constant feed concentration .

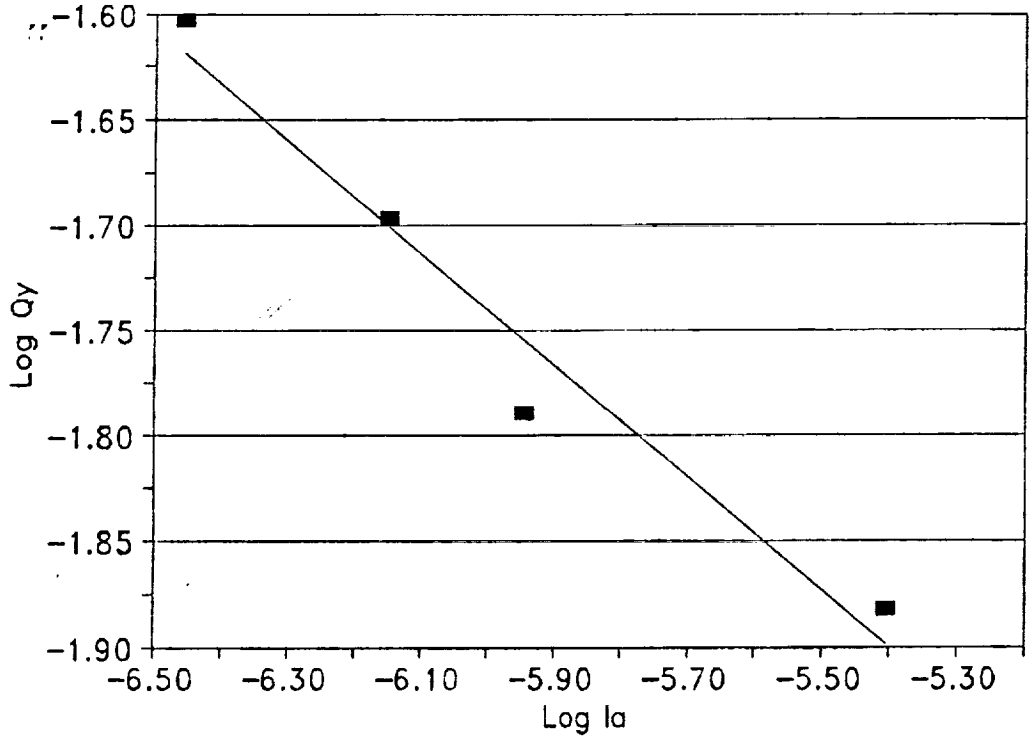

Figure 7: Quantum yield vs. irradiance; acetone conversion at constant acetone feed concentration.

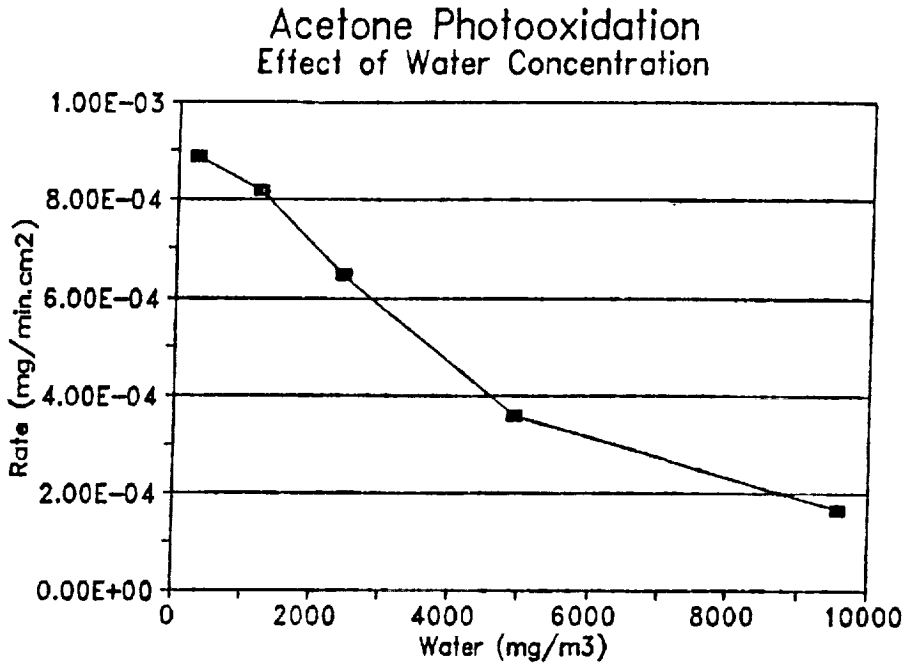

Figure 8: Rate of acetone photocatalyzed oxidation vs. feed water vapor concentration; acetone feed concentration = constant.

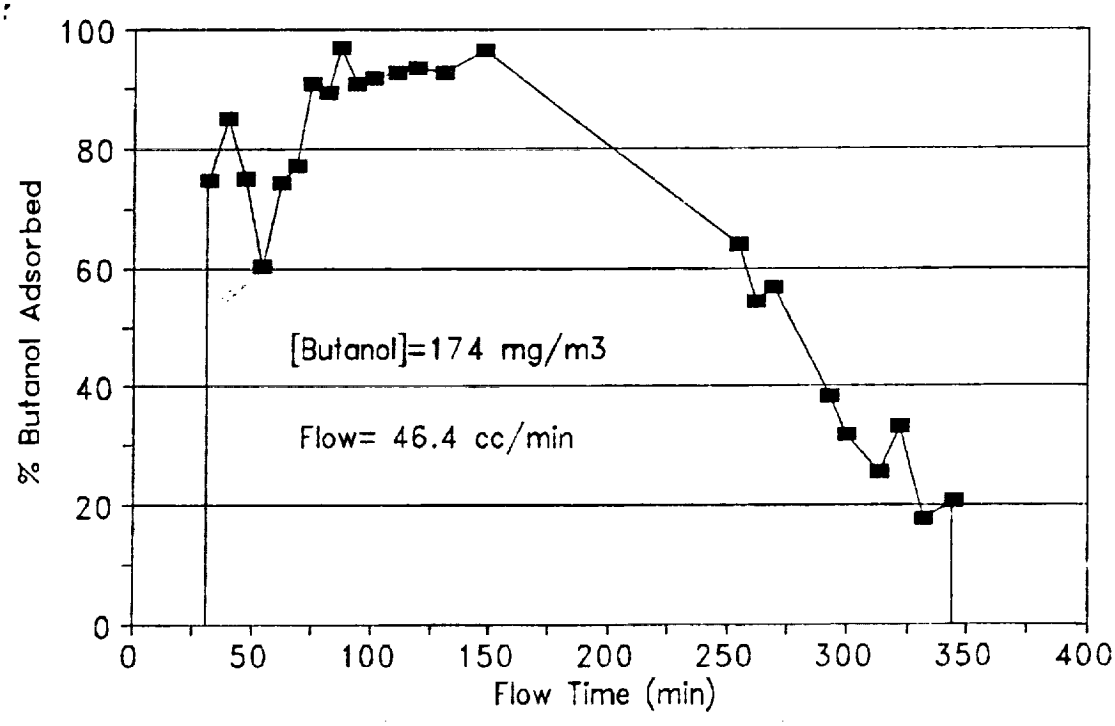

Figure 9: Percent butanol adsorbed vs. time of air/n-butanol flow; dark conditions.

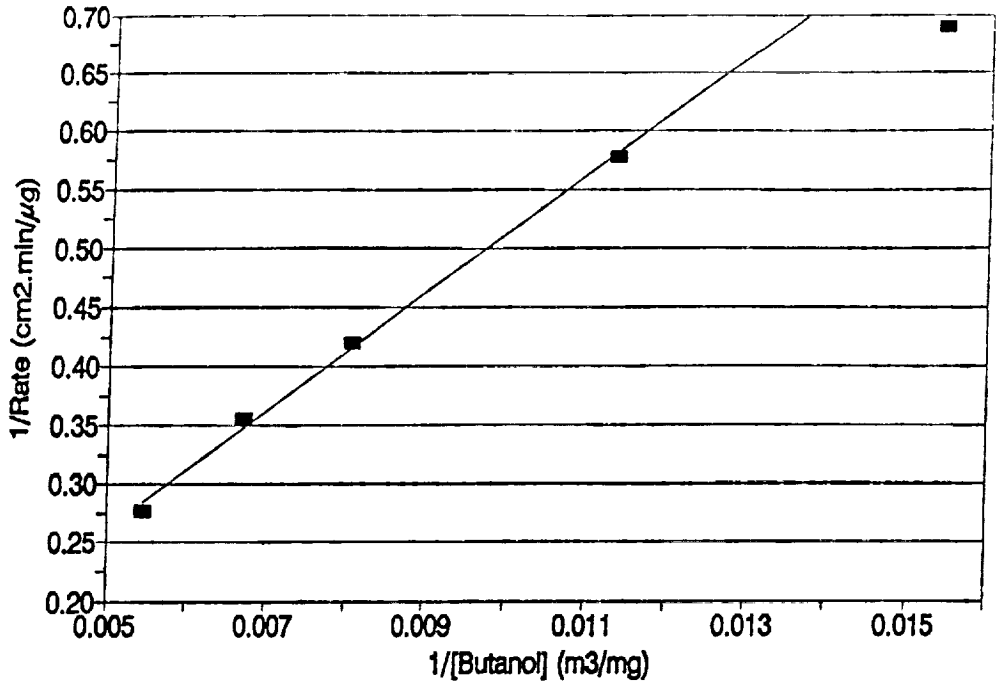

Figure 10: Reciprocal rate of butanol conversion vs. reciprocal of butanol feed concentration.

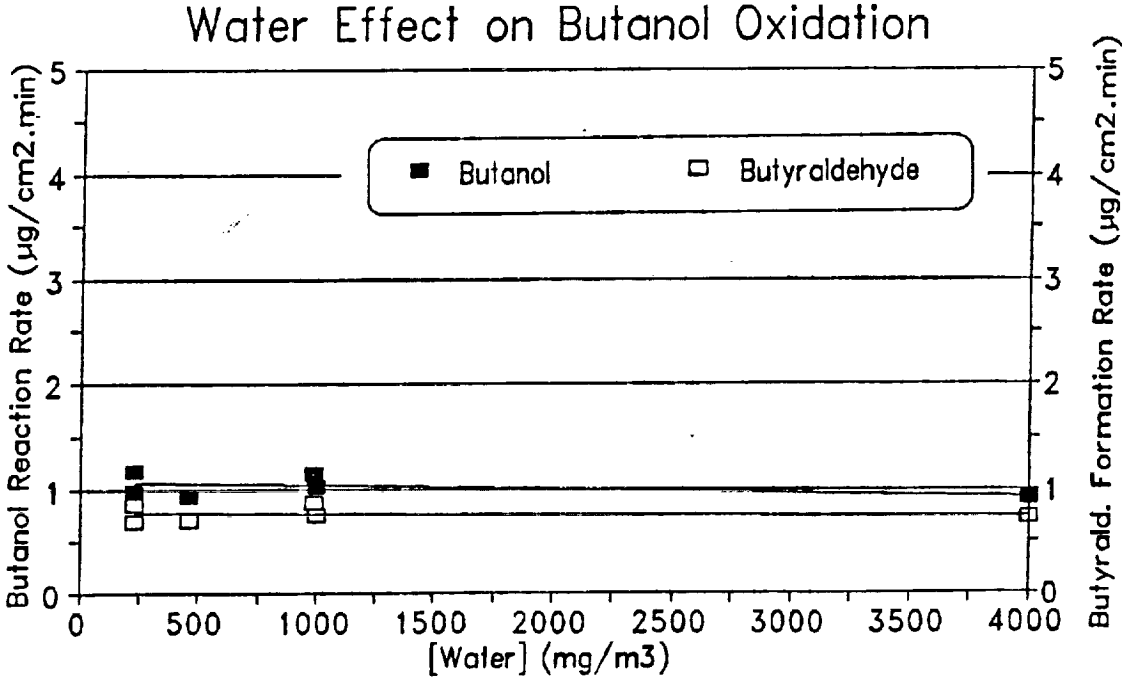

Figure 11: Butanol reaction rate(left) and buteraldehyde formation rate(right) vs. water vapor content of feed.

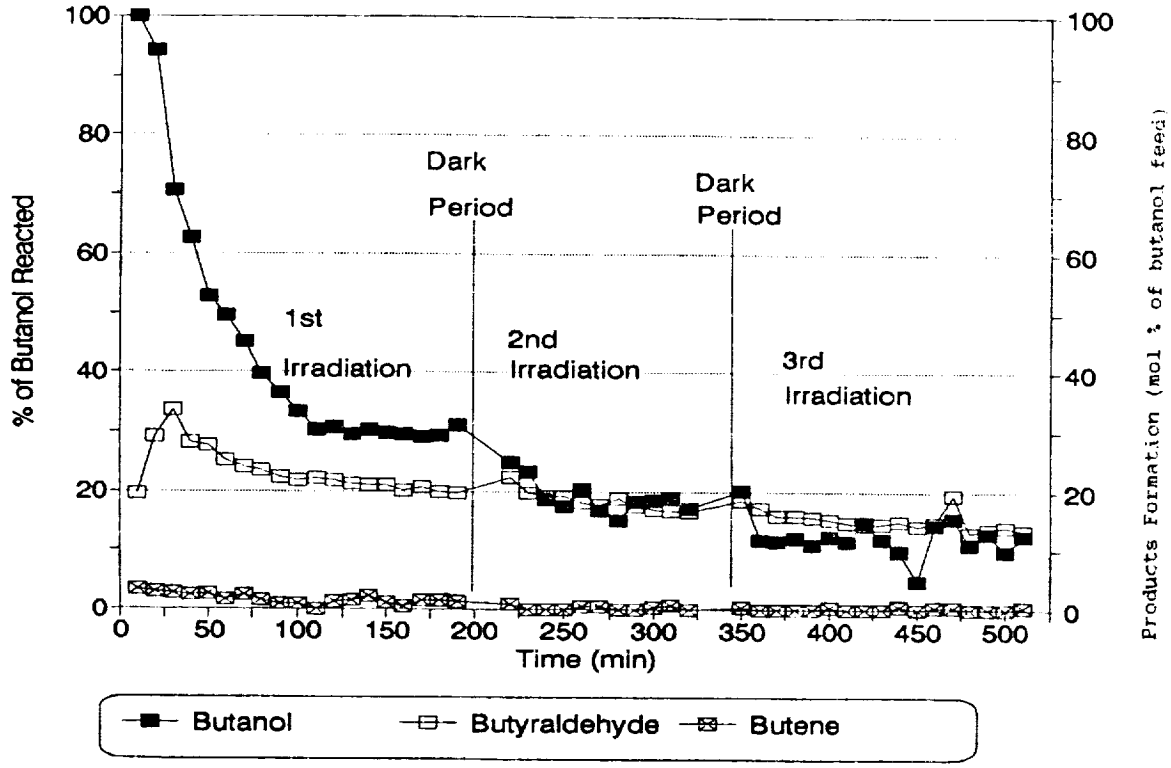

Figure 12: Butanol percent reacted (left) and product formed as percent of butanol fed (right) vs. reaction time; time of dark periods not included. (Feed butanol = 260 mg/m^3)

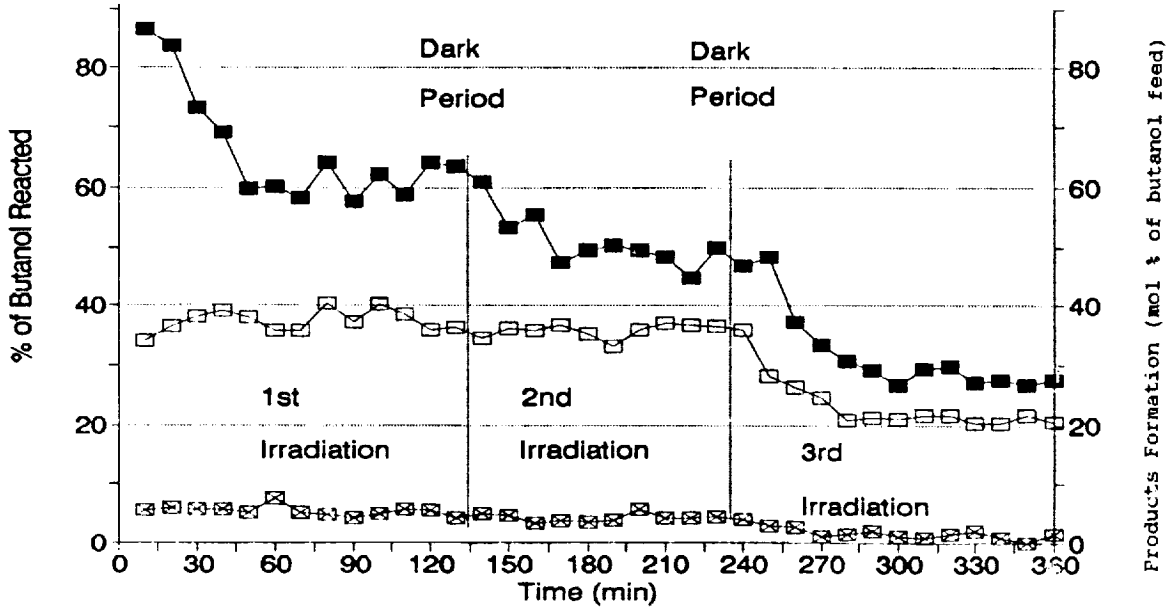

Figure 13: Butanol percent reacted (left) and products formed as percent of butanol fed (right) vs. reaction time; dark time period not shown. (Feed butanol concentration = 140 mg/m^3)

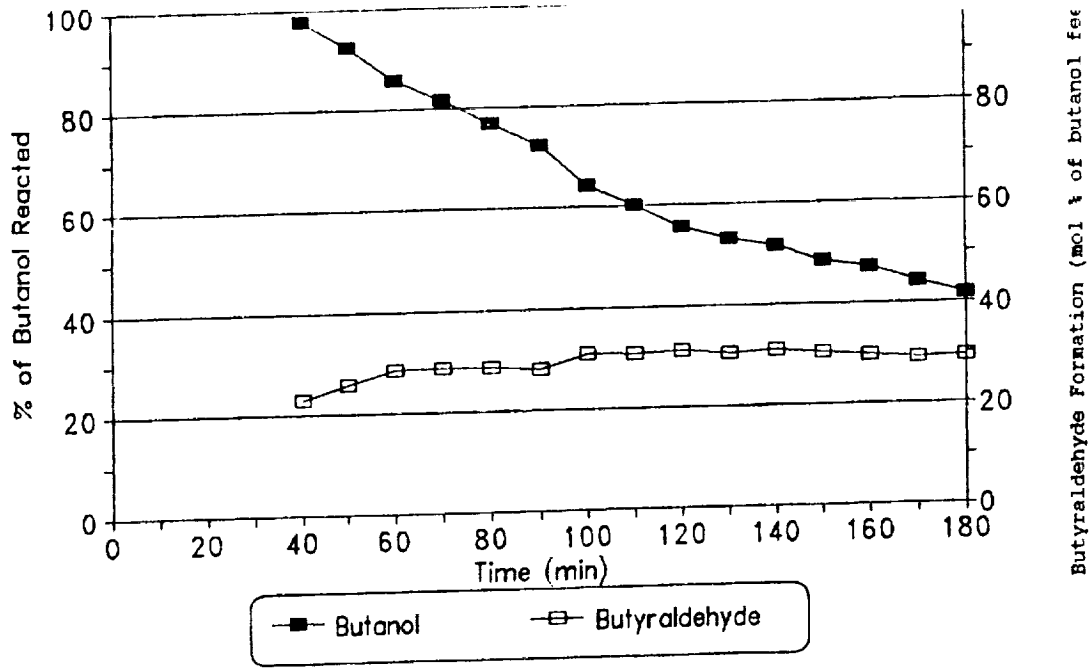

Figure 14: Deactivation: Percent butanol converted vs. time of reaction.

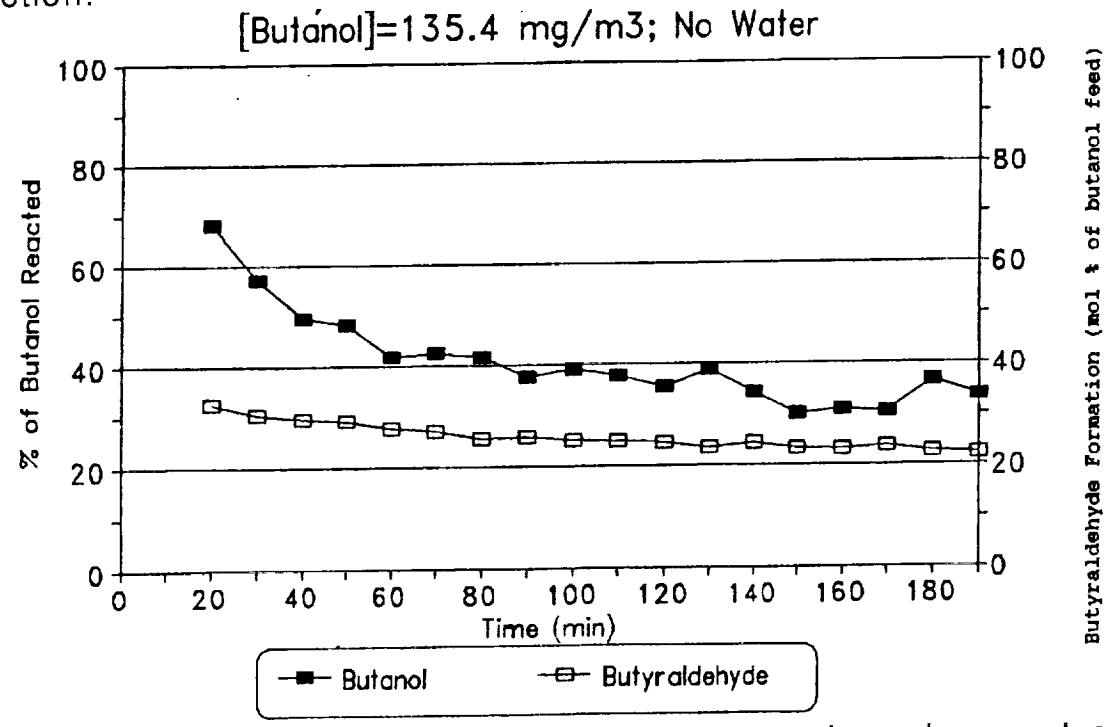

Figure 15: Deactivation: Percent of butanol removal and percent of buteraldehyde formed vs. reaction time.

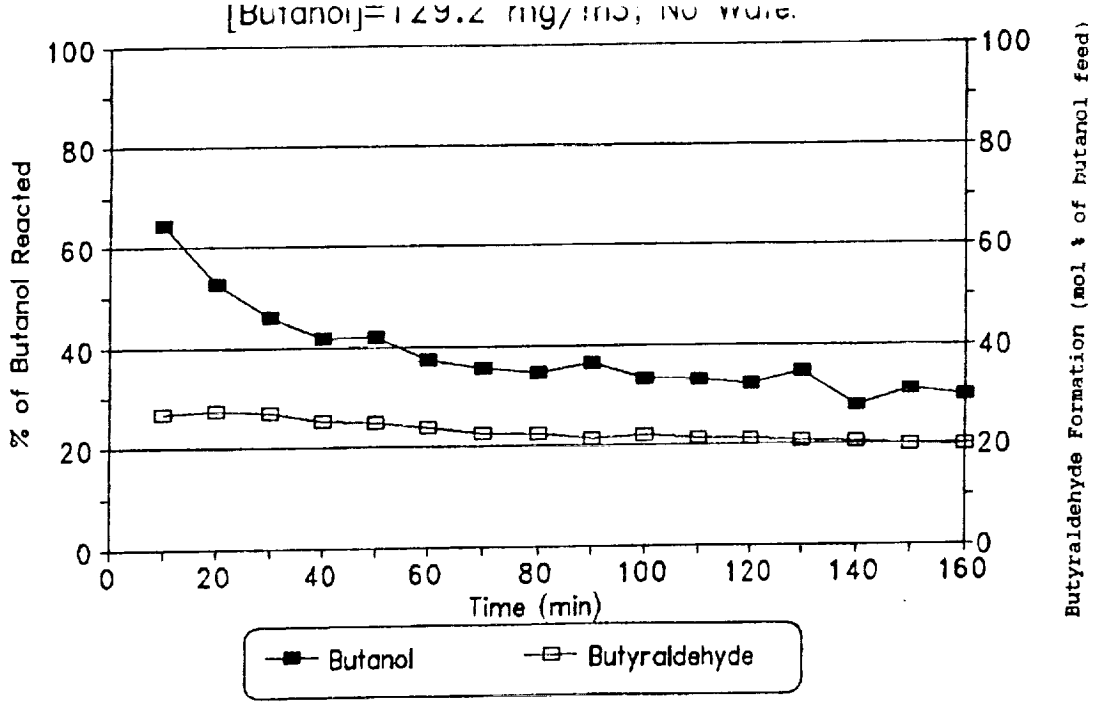

Figure 16: Deactivation: Percent butanol converted and percent of buteraldehyde formed vs. reaction time.

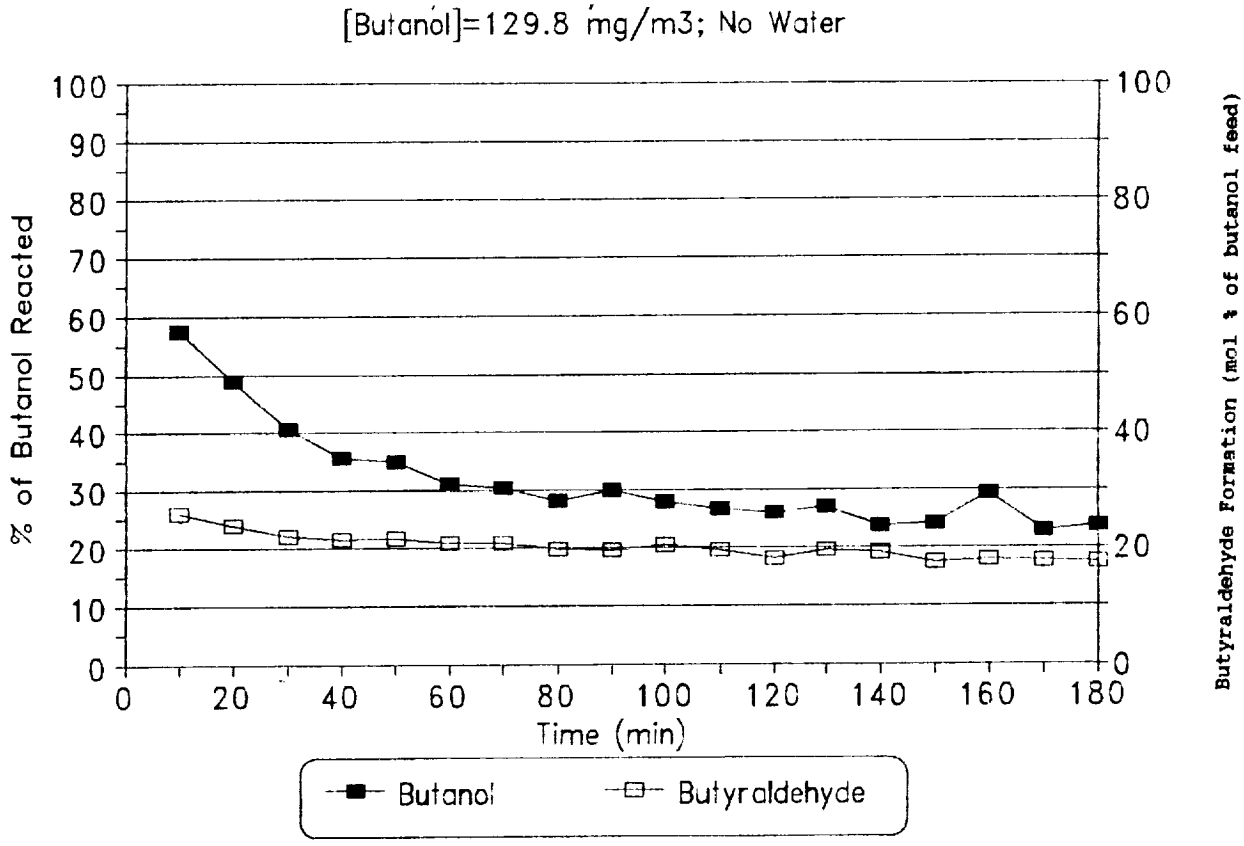

Figure 17: Deactivation: Percent butanol reacted and buteraldehyde formed vs. reaction time.

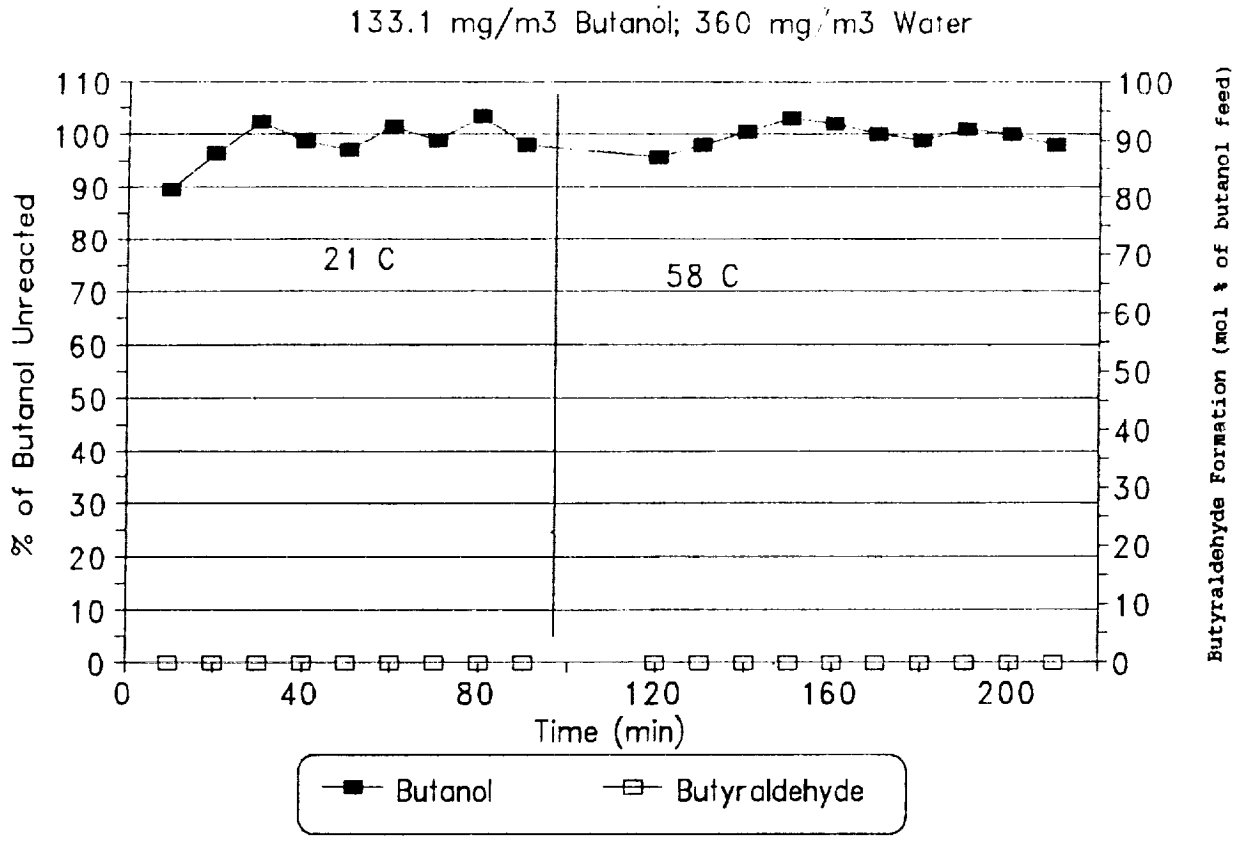

Figure 18: Test for dark reaction activity: percent of butanol reacted (left) and percent of buteraldehyde formed(right) vs reaction time.

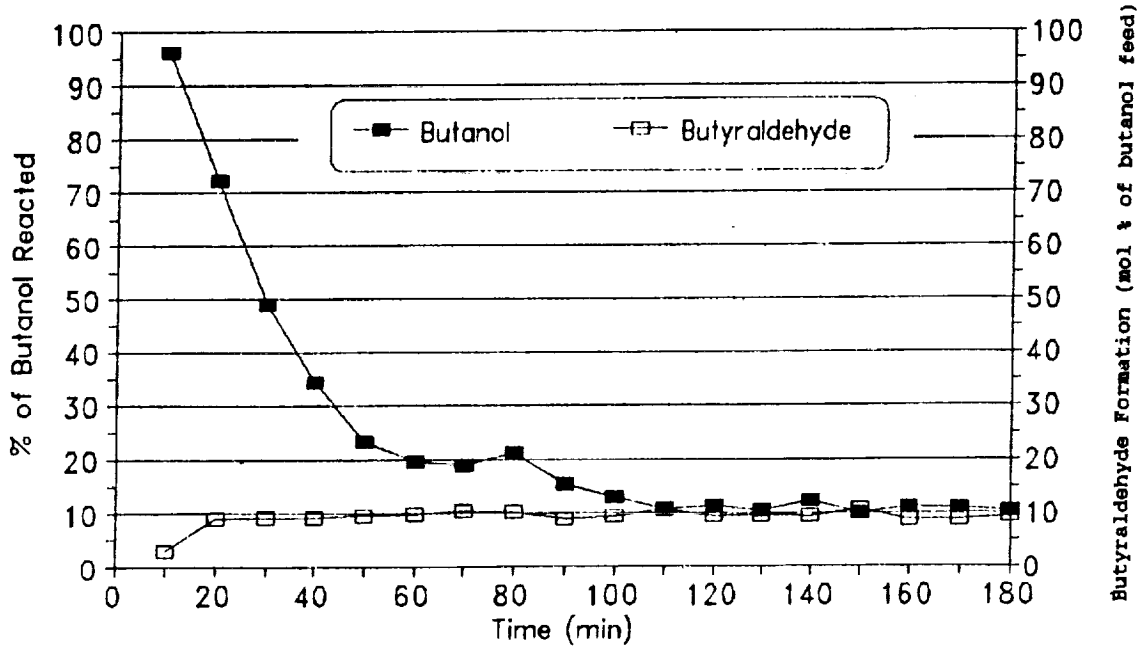

Figure 19: Influence of temperature on deactivation: percent butanol converted and buteraldehyde formed vs. reaction time at 75-80^{o}C.

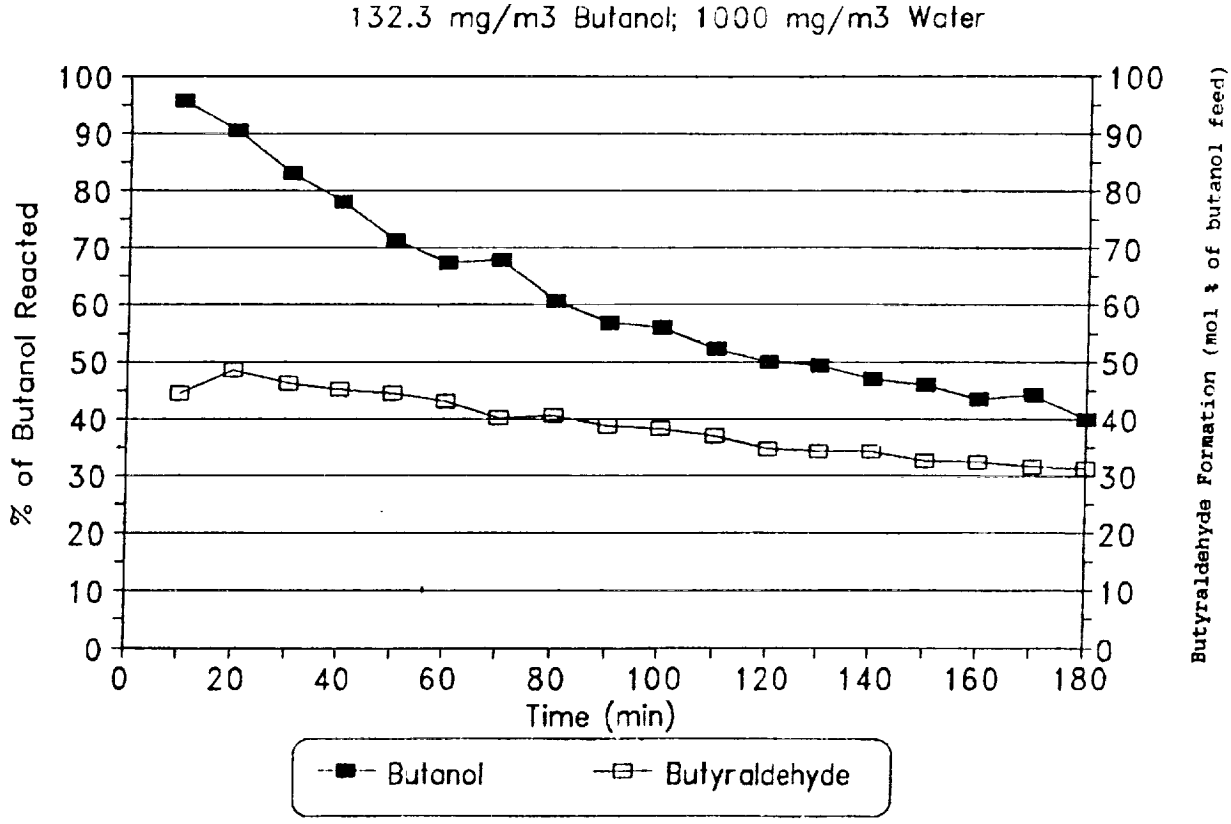

Figure 20: Effect of temperature on deactivation: conversion of butanol and formation of buteraldehyde vs. reaction time: T = 61-62°C.

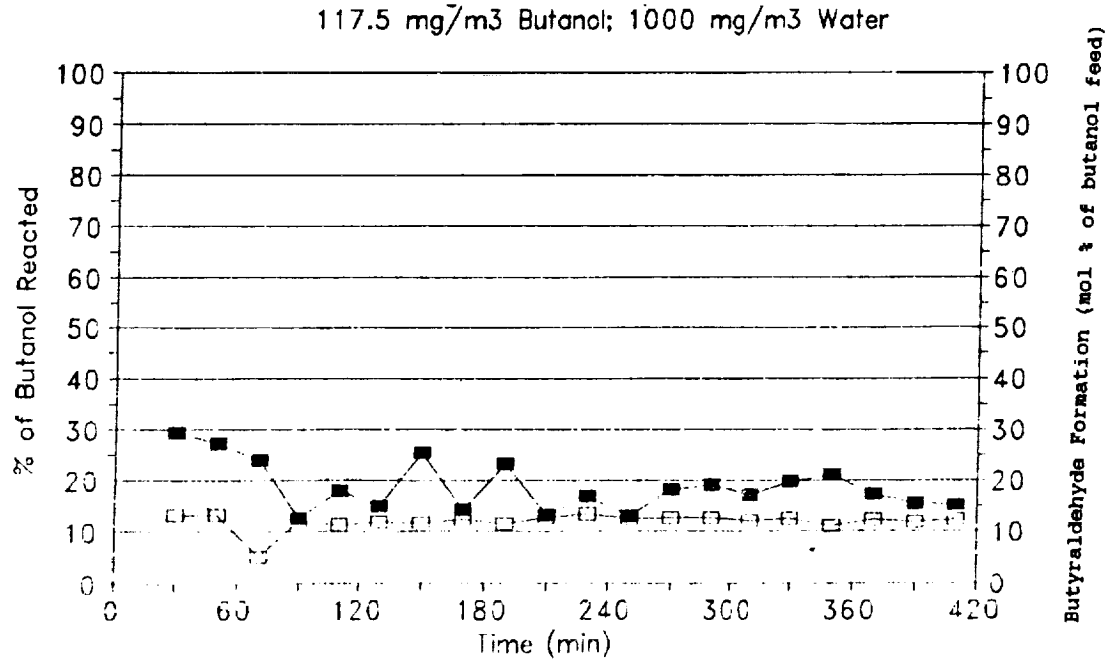

Figure 21: Long time irradiation: butanol conversion and buteraldehyde formation vs. reaction time. T = 22-25 °C.